Available online at www.sciencedirect.com

ScienceDirect

Materials Today: Proceedings 19 (2019) 1091–1098

materialstoday: PROCEEDINGS

www.materialstoday.com/proceedings

BraMat 2019

Microstructure, phase transformations and properties' evaluation of Al-Si-Ni metastable alloys

Alexandra Nitoi[1,*], Tibor Bedo[1], Bela Varga[1], Mihai Alin Pop[1], Daniel Munteanu[1]

[1]*Transilvania University of Brasov, Material Science Department, 29 Eroilor Blvd., 500036, Brasov, Romania*

Abstract

Additive manufacturing is a technology which has the potential to replace conventional casting methods. The versatility delivered by this process is of great interest, mainly due to the capacity to manufacture complex shapes, as well as the multitude of materials which can be used. Generally, the metallic powders used in additive manufacturing are obtained by gas atomization, meaning that the alloys solidify rapidly from the melt pool. This phenomenon determines both the improvement of mechanical properties, due to the finishing of the structure, as well as potentially obtaining metastable structures in the form of supersaturated or amorphous/nano solid solutions. Aluminium-based metallic glasses are of interest due to their combined high specific strength to weight ratio, good ductility and superior corrosion resistance. The paper presents results concerning the microstructural evolution for bulk, melt-spun ribbons. Al-Si-Ni alloys (Al_{70}-Si_{18}-Ni_{12}, Al_{68}-Si_{18}-Ni_{14},Al_{66}-Si_{18}-Ni_{16}). It was observed that structural transformations during heating, starting from metastable structures (melt-spun ribbons), generate significant amounts of energy. This phenomenon could be of practical importance in the use of metallic powders in additive manufacturing technology.

Selection and peer-review under responsibility of the 11th International Conference on Materials Science & Engineering, BraMat 2019

Keywords:metastable alloys, melt spinning; exothermal phase transformation.

1. Introduction

Additive manufacturing [AM] is based on using computer-aided-design (CAD) software, which allows one to design and manufacture hard-to-obtain an intricate geometric shapes, otherwise difficult to obtain by other means of

* Corresponding author. Tel.: +40 0736852375.
E-mail address: alexandra.nitoi@unitbv.ro

Selection and peer-review under responsibility of the 11th International Conference on Materials Science & Engineering, BraMat 2019

manufacturing. Three-dimensional printing (3D-printing), also known as additive manufacturing (AM) or rapid prototyping has several applications in various areas, from the automotive sector, to the aerospace, and beyond [1]. Lightweight materials, including Al–Si alloys, are used due to their properties, such as high strength to weight ratio and good corrosion resistance [2]. Due to its high fluidity, low shrinkage and low density, Si is one of the major alloying elements in Al alloys. It should be considered that with increasing Si content, the machinability of the aluminum alloy decreases, due to the fragile nature of the alloy [3]. However, Si represents an important element needed for the phenomenon of amorphization. H. Minouei et al. reported that increasing the Si content to 5 and 10 at% in Ni-Nb-Si-type alloys, leads to solid state phase transformations, observed as exothermic peaks during thermal analysis, which may indicate a delay in the formation of amorphous phase after the formation of solid solution [4].

Generally, the powders used in AM processes are obtained by atomization, which is one of the fast-solidification methods. Rapid solidification can be done in different ways, such as: chilling methods (melt-spinning) and atomization methods (gas, water and centrifugal atomization) [5]. Rapid solidification of metallic alloys confers a modification of mechanical properties in contrast with the conventionally processed alloys, due to the structural refinement during cooling, up to the nanometric scale or even further, due to the formation of amorphous materials. These metastable materials and amorphous alloys could contribute to reduce the energy consumption of the AM process [6], due to potential exothermic phase transformations during heating which could contribute to lower the sintering or melting temperature.

To date, reports have can be found in the literature, concerning the microstructure and mechanical properties of Al-Si, Al-Si-Fe and Al-Si-Cu ribbons produced by melt-spinning. M. Rajabi noticed a higher hardness of the materials compared with the conventionally cast alloys. It was reported that the mechanical strength was improved by mixing Al–20Si–5Fe ribbons with Cu, Ni, and Cr. Higher content of Ni leads to better mechanical behaviour at elevated temperatures [7].

Concerning the development of Al-Si-Ni metallic glasses or metastable alloys, the literature is significantly less scarce. Alberta Aversa et al. presents results concerning the mechanical properties and microstructure for Al-Si-Ni materials, produced via selective laser melting (SLM). The report mentions the mixing of AlSi10Mg powders with pure Ni powders, followed by sintering. In this particular case, the addition on nickel leads to higher hardness due to the formation of Al_3Ni precipitates [8]. Tawfik compared the mechanical properties of a melt spun Al-Si-Ni alloy and as-cast commercial alloys with similar compositions. Rapid solidification conferred the specimens a 40% higher ultimate tensile strength [UTS], the UTS values for Al-16Si and Al-12.5Si-1Ni are higher, while that for Al-12.5Si-1 Mg is the same or even lower [9]. However, we need to mention that the manufacture procedure is different in these reports, compared to the one presented herein. Moreover, E. Karakose et al. analysed the microstructural evolution and microhardness of a melt-spun Al–6Ni–2Cu–1Si (in wt.%) alloy. It was observed that the grain morphology in the ribbons depends on the variation of the cooling rates. Microhardness values of the melt-spun Al–Ni–Cu–Si alloy were higher than the values obtained on conventionally cast samples, due to the formation of Al_3Ni intermetallic phase, which contributed to improve the hardness at the expense of its ductility [10].

This paper presents the structure evolution for melt-spun ribbons of Al-Si-Ni alloys ($Al_{70}Si_{18}Ni_{12}$, $Al_{68}Si_{18}Ni_{14}$, $Al_{66}Si_{18}Ni_{16}$), compared to their bulk, as-cast counterpart. The silicon content was kept the same between compositions, while the aluminum and nickel contents were varied, in order to assess possible mechanical property variations, related to either the chemical composition, or the processing parameters (cooling rates).

2. Experimental details.

Preliminary Al-Si-Ni alloys, namely $Al_{66}Si_{18}Ni_{16}$, $Al_{68}Si_{18}Ni_{14}$, $Al_{70}Si_{18}Ni_{12}$, were obtained by gravity casting. The chemical compositions and proportions between elements were chosen according to the ternary Al-Si-Ni equilibrium phase diagram. It was reported that the chemical compositions situated in the Al-rich corner of the Al-Si-Ni ternary diagram can be relatively easily obtained in amorphous form. Consequently, the compositions presented herein were chosen from this particular region. The alloys were developed in a silicon carbide resistor furnace, in graphite and steel crucibles, under a protective flux layer, to avoid oxidation of the melt and to remove other impurities.

The thin alloy ribbons were obtained by melt-spinning. As mentioned previously, the melt-spinning technique facilitates obtaining very high cooling rates, which translate to either the refinement of the structure, or the possibility to obtain amorphous materials. To further assess the effect of the cooling rate on the melt-spun ribbon

structural development and consequently on the material properties, two rotation speeds were used for the copper cooling wheel, namely 32m/s and 15m/s, resulting in a total of nine sample configurations, as function of the chemical composition and cooling rate: as-cast bulk samples, melt-spun ribbons obtained with a lower cooling rate, melt-spun ribbons with a higher cooling rate. The chemical compositions, both in %at and % weight, as well as the symbol used in the manuscript, are presented in Table 1.

Table 1. Al-Si-Ni alloy compositions.

% at	% weight	symbol
$Al_{66}Si_{18}$-Ni_{16}	Al55,21-Si15,67-Ni29,12	Ni16
Al_{68}-Si_{18}-Ni_{14}	Al58,02-Si15,99-Ni25,99	Ni14
Al_{70}-Si_{18}-Ni_{12}	Al60,95-Si16,32-Ni22,73	Ni12

After the casting and melt-spinning processes, samples were embedded in resin, and further mechanically polished, to a mirror-like finish. The structural analysis was performed with a Nikon metallographic microscope (up to 1000 × magnification). Several magnifications were used, in order to better observe the phases of the Al-Si-Ni samples, in bulk and melt-spun form.

The structural stability was assessed by thermal analysis, namely differential thermal analysis (DTA) with STA 449 F3 JUPITER (NETZSCH), up to the maximum temperature of 900 °C in a nitrogen atmosphere, with a heating/cooling rate of 10 °C/min. The data processing was done using the NETZSCH Proteus Analysis software.

In order to assess some of the mechanical properties of the samples, microhardness tests were performed with a FM 700 microhardness tester, carried out with 1gf load, and a dwell period of 10 s, in order to minimize as much as possible the elastic recoil of the material. Moreover, instrumented indentation was performed using a NHT^2 head from CSM Instruments: with the following protocol: maximum applied load 20mN, loading rate 60mN/min, unloading rate 180 mN/min, dwell period 2s. The results of interest were Hit (indentation hardness) and Eit (indentation elastic modulus). At least 10 indentations were performed on each sample, and the results were averaged.

3. Results and discussions

In the optical micrographs, shown in figure 1, the structure of the aluminum-based alloys can be observed, as function of the casting procedure (as-cast or melt-spun with two different cooling rates), and as function of the chemical composition. The as-cast structure of the $Al_{70}Si_{18}Ni_{12}$ alloy, shown in figure 1(1-a), shows rather large crystalline regions, with clearly distinguished phases. It is obvious that as the cooling rate is lower the phases can be seen better. The cooling rate was relatively slow, in as much that it could be considered an equilibrium solidification process, which corresponds to the separation from the liquid phase of the intermetallic compound Al_3Ni and of the eutectic, according to the following relation: $L \rightarrow Al_3Ni + (Si+\alpha\text{-}A)$. Increasing the cooling rate, for the 15 m/s melt-spun ribbons, leads to a structural refinement, noticed in figure 1 (1-b). Smaller phases can be observed for the same magnification, thus confirming the structural refinement. However, the intermetallic compound and the silicon crystals are still visible. Further increasing the cooling rate leads to a significant structural refinement, seen in figure 1(1-c). Oxide particles from the mechanical polishing can be seen. Otherwise, no granular structure could be observed, regardless of the magnification. A somewhat similar structural evolution can be observed for the remaining compositions, namely $Al_{68}Si_{18}Ni_{14}$ and $Al_{66}Si_{18}Ni_{16}$: the bulk as cast alloys exhibit large crystalline grains composed of the intermetallic compound and silicon, embedded in the eutectic matrix. However, a few ley differences could be observed. The melt-spun ribbons, regardless of the cooling rate during the melt-spinning process, seem to be increasingly fragile, noticed from the large fractures which occurred due to the mechanical polishing process. This behavior could be linked to the increasing nickel content in the alloys. Choi et al. studied the high temperature tensile deformation behavior of new heat resistant aluminum alloy with added nickel, and noticed a strong interconnected three-dimensional structure with Al_3Ni and eutectic silicon [11]. The interconnectivity was correlated with the quantity of the Ni-rich compounds present in the eutectic matrix. Moreover, with increasing nickel content the structural refinement seems to be less pronounced, even for the higher melt-spinning speeds, as can be seen in figures 1 (2-c) and 1 (3-c), compared to figure 1 (1-c).

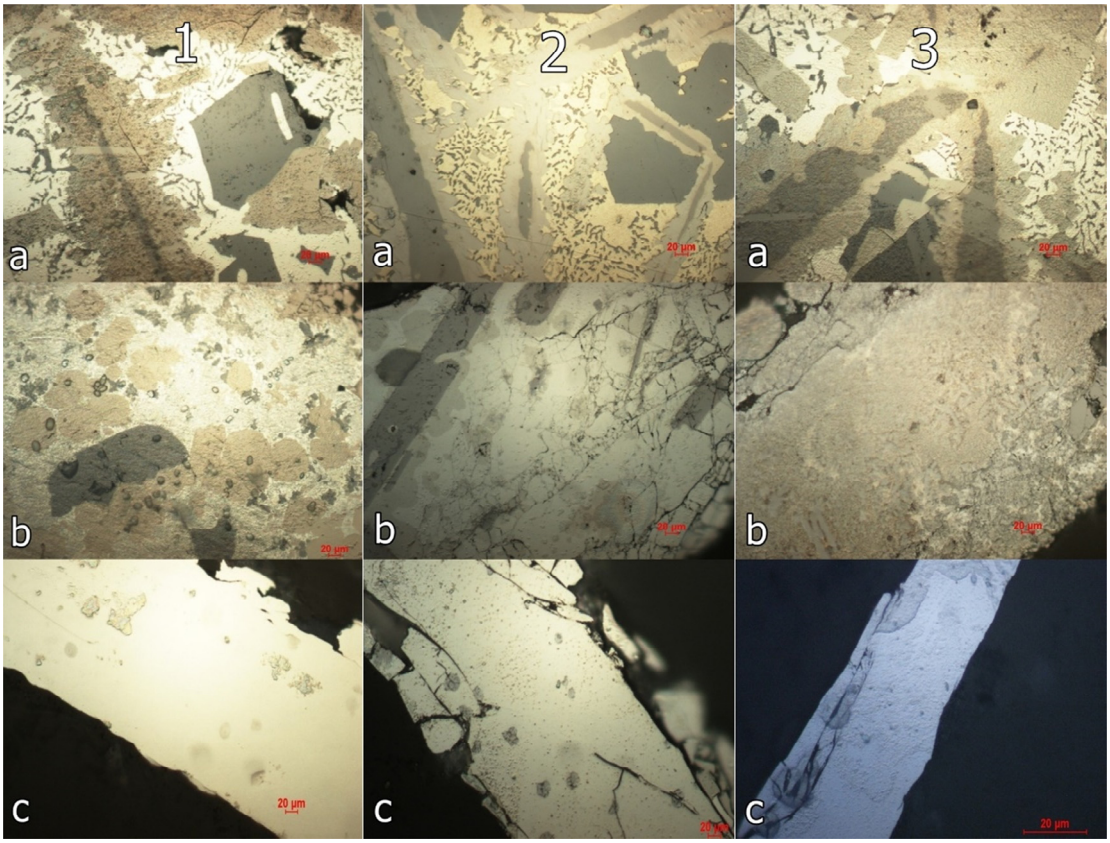

Fig. 1. 1 - Optical micrographs of the $Al_{70}Si_{18}Ni_{12}$ alloys: (a) bulk; (b) v=15m/s; (c) v=32 m/s; 2 - Optical micrographs of the $Al_{68}Si_{18}Ni_{14}$ alloys: (a) bulk; (b) v=15m/s; (c) v=32 m/s; 3 - Optical micrographs of the $Al_{66}Si_{18}Ni_{16}$ alloys: (a) bulk; (b) v=15m/s; (c) v=32m/s.

Nanostructured or amorphous materials could exhibit certain phase transformations upon heating, measurable as exothermal or endothermal peaks, which occur during the heating of the material in question. Following the thermal analysis procedure, the results are shown in figures 2 and 3, as function of the chemical composition (figure 2), and of the melt-spinning rotation speed (cooling rate) (figure 3). It can be noticed that with the increase of the cooling rate several exothermic peaks appear, especially for the higher cooling rate melt-spun ribbons. It can be observed that, as function of the chemical composition, once the nickel content is increased, the exothermal peaks develop at higher heating temperatures. However, the intensity and the peak area seems to decrease with higher nickel content. The endothermal peaks are generally related to melting phenomena occurring in the material. If one considers the ternary phase diagram for the Al-Si-Ni system, three melting instances should take place, as function of the temperature and chemical composition, namely: firstly, the eutectic, at temperatures between 557 °C-569 °C, secondly the lower nickel content Al_3Ni intermetallic compound between 648 °C-661 °C, lastly the higher nickel content $Ni_2(Al_{1-x}Si_x)_3$-type intermetallic compound, between 764 °C -767 °C. Observing the variation from the graphs presented in figure 2, the third phase transformation does not occur for the $Al_{70}Si_{18}Ni_{12}$ alloy, it is slightly noticed for the $Al_{68}Si_{18}Ni_{14}$ alloy, and even more so for the $Al_{66}Si_{18}Ni_{16}$ alloy, thus confirming the influence of the nickel content on the formation of the $Ni_2(Al_{1-x}Si_x)_3$-type intermetallic compound.

Further analyzing figure 3, where the thermal transformations for the three alloy compositions are compared as function of the cooling rate, due to the processing stage by melt spinning with two different peripheral speeds, one can observe that the for higher nickel content the exothermal phase transformations are occurring at higher temperatures. However, the energy release is inversely proportional to the nickel content, observed from the total peak area for the exothermal transformations, which is noticeably higher for the $Al_{70}Si_{18}Ni_{12}$ alloy, processed with 32 m/s peripheral speed. These exothermal transformations could potentially decrease the necessary energy input for melting and sintering the alloy granules, during additive manufacturing processes.

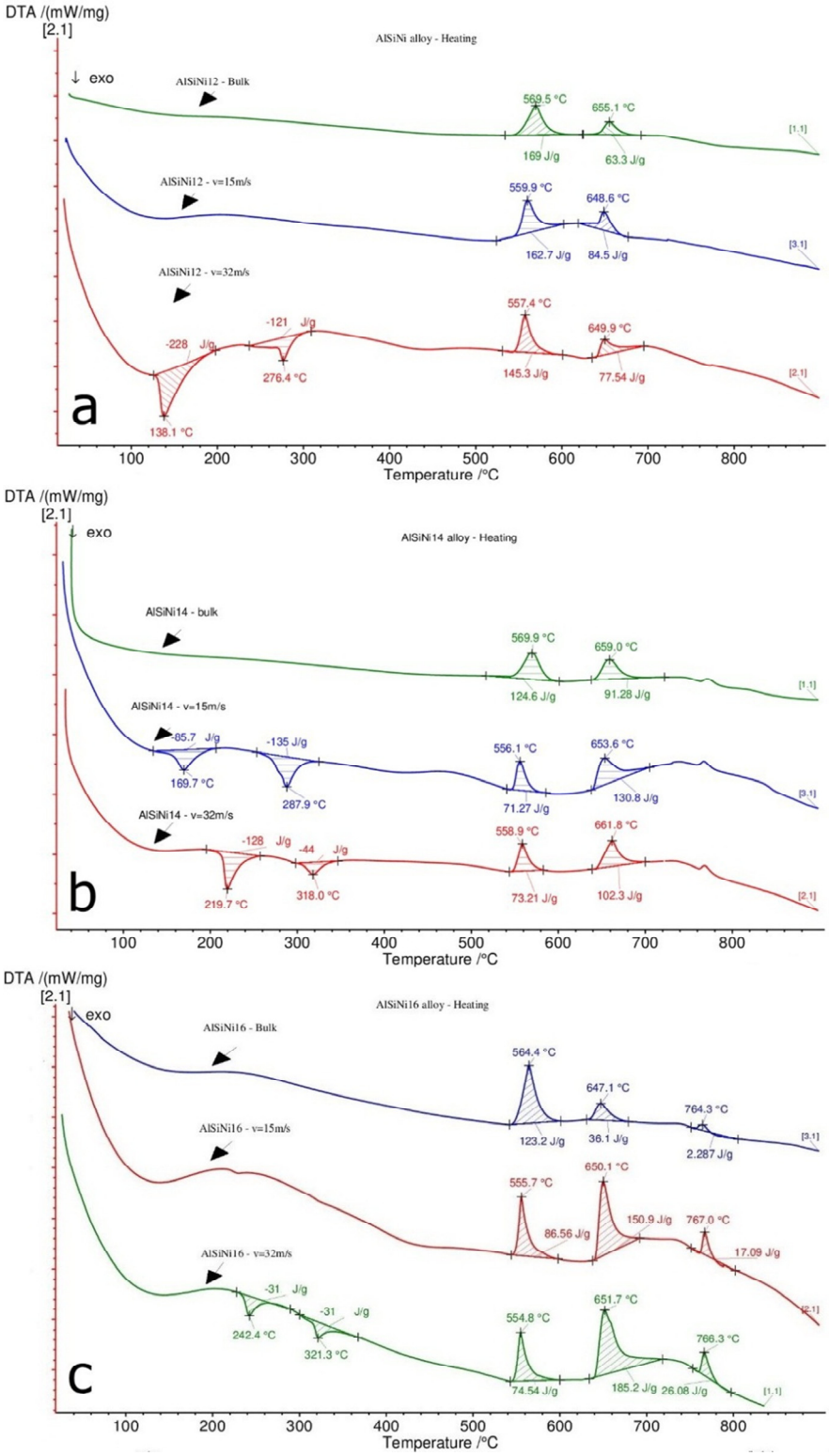

Fig. 2. Differential thermal analysis: (a). $Al_{70}Si_{18}Ni_{12}$; (b). $Al_{68}Si_{18}Ni_{14}$; (c). $Al_{66}Si_{18}Ni_{16}$- Bulk, v=15m/s, v=32m/s- DTA.

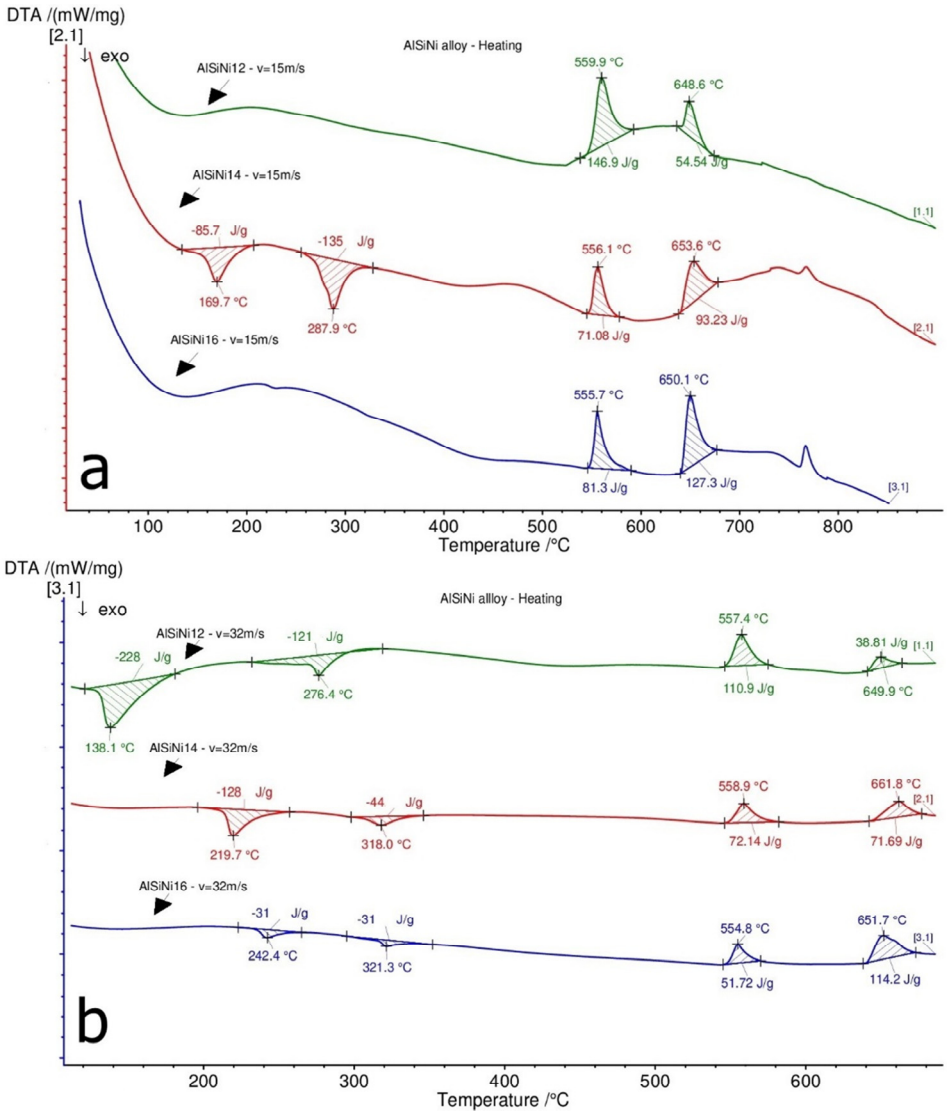

Fig. 3. Differential thermal analysis comparison, as function of the chemical compositions, for the melt-spun ribbons: (a). $Al_{70}Si_{18}Ni_{12}$; $Al_{68}Si_{18}Ni_{14}$; $Al_{66}Si_{18}Ni_{16}$- v=15 m/s- DTA; (b). $Al_{70}Si_{18}Ni_{12}$; $Al_{68}Si_{18}Ni_{14}$; $Al_{66}Si_{18}Ni_{16}$- v=32 m/s- DTA.

Considering that the applicability of a newly proposed alloy is highly dependent on its properties, the behaviour of the Al-Si-Ni alloys proposed herein was estimated through localized hardness measurements, through microindentation, as well as through instrumented indentation. Consequently, one of the purposes of the present work was to reveal the relationships between the solidification processing parameters and the hardness of the Al-Si-Ni alloys. Figure 4 represents the variation of the Vickers microhardness, obtained on the bulk $Al_{70}Si_{18}Ni_{12}$, $Al_{68}Si_{18}Ni_{14}$, and $Al_{66}Si_{18}Ni_{16}$ alloys, measured on the distinct phases which were observed during the optical microscopy structural analysis. The microhardness of the eutectic phase does not change significantly between compositions, a phenomenon which should be expected, considering that the chemical composition of the eutectic phase would not change. However, considering the Al_3Ni-like intermetallic compounds, the hardness variation is significantly larger. Comparing the $Al_{70}Si_{18}Ni_{12}$ and the $Al_{66}Si_{18}Ni_{16}$ alloys, the observation that the hardness of the intermetallic compound is relatively higher should be correlated to the higher nickel content, which would mean that a larger proportion of the material is represented by the intermetallic compound, and to the higher possibility of formation of the $Ni_2(Al_{1-x}Si_x)_3$-type intermetallic compound. The peculiar result obtained on the bulk sample from

the $Al_{68}Si_{18}Ni_{14}$ alloy composition could be related to the possibility of measuring a particular inhomogeneous region, even if the measurements were repeated in several locations, in order to minimize the measuring error. In order to clarify the situation, further instrumented indentation measurements were performed on the melt-spun ribbons. Figure 5 exhibits the loading-unloading curves obtained on the melt-spun ribbons, processed with two cooling rates, extrapolated from the two rotation speeds of 15 m/s and 32 m/s.

A certain degree of variation is clearly noticed between samples, without an obvious correlation to the chemical composition alone. If one considers the hardness of a material, which represents its capacity to resist to plastic deformation, several factors can influence this characteristic. Generally, it is assumed that the specimen material could be stress-free before the measurements.

However, in many materials, stresses, tensile or compressive, may be present within the specimen as a result of processing, (temperature induced, as is the case of fast-cooling processes) or sample surface preparation (cold working from mechanical polishing). Consequently, the presence of residual stress can influence the results of instrumented indentation experiments. Moreover, due to slip resistance of the atoms during the indentation loading different hardness levels could result.

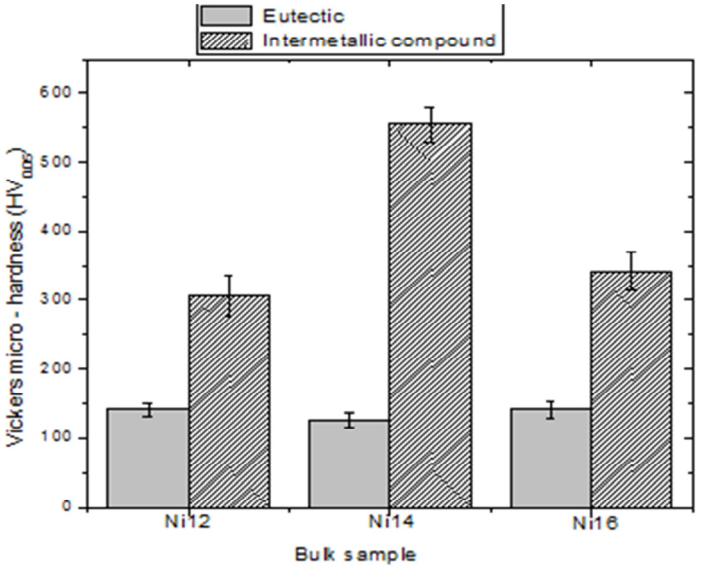

Fig. 4. Micro-hardness values obtained on the $Al_{70}Si_{18}Ni_{12}$, $Al_{68}Si_{18}Ni_{14}$, and $Al_{66}Si_{18}Ni_{16}$ alloy bulk samples.

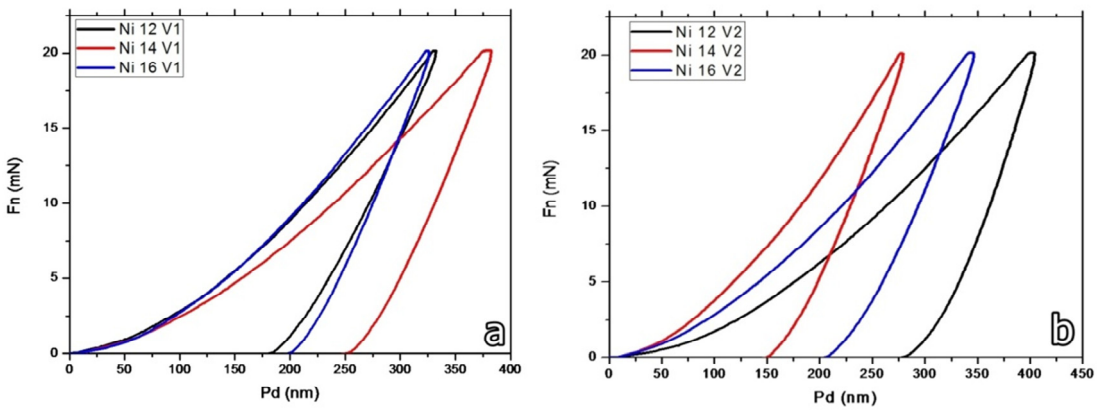

Fig. 5. Indentation alloy ribbons: (a). $Al_{70}Si_{18}Ni_{12}$;$Al_{68}Si_{18}Ni_{14}$;$Al_{66}Si_{18}Ni_{16}$v=32m/s; (b). $Al_{70}Si_{18}Ni_{12}$;$Al_{68}Si_{18}Ni_{14}$; $Al_{66}Si_{18}Ni_{16}$ v=15m/s.

4. Conclusions

In this work, the microstructure, thermal analysis and mechanical properties of Al-Si-Ni alloys were investigated. From the experimental results, the following conclusions can be drawn: for all the alloys studied, rapid solidification resulted in a significant structural refinement, compared to the alloys processed by conventional means. Solid state phase transformations were observed during heating, extrapolated from the highly exothermal peaks, on the samples processed by fast solidification means (melt-spinning). The occurrence of these exothermal peaks could have implications in regards to the possibility of processing these materials during additive manufacturing with lower energy input. Indentation analyses carried out on the Al-Si-Ni samples demonstrated that the increase of the hardness is mainly due to the Al_3Ni precipitates. However, the formation of these intermetallic compounds could have a detrimental effect on the fragility of the alloys.

Acknowledgements

This project has received funding from the European Union's Horizon 2020 research and innovation programme under grant agreement No. 723699. We hereby acknowledge the structural funds project PRO-DD (POS-CCE, O.2.2.1., ID 123, SMIS 2637, ctr. No 11/2009) for providing the infrastructure used in this work.

References

[1] M. Attaran, The rise of 3-D printing: The advantages of additive manufacturing over traditional manufacturing, Business Horizons, 60 (2017) 677-688.
[2] Z. Chen, Y. Lei, H. Zhang, Structure and properties of nanostructured A357 alloy produced by melt spinning compared with direct chill ingot, Journal of Alloys and Compounds, 509 (2011) 7473-7477.
[3] S. Arthanari, Jae Cheol Jang, Kwang Seon Shin, Corrosion studies of high pressure die-cast Al-Si-Ni and Al-Si-Ni-Cu alloys, Journal of Alloys and Compounds 749 (2018) 146-154.
[4] H. Minouei, Amorphization and Nanocrystallization of Ni–Nb-Si Alloys,Materials Science and Engineering: A 682 (2017) 396-401.
[5] C.L. Xu, H.Y. Wang, F. Qiu, Y.F. Yang, Q.C. Jiang, Cooling rate and microstructure of rapidly solidified Al–20 wt.% Si alloy, Materials Science and Engineering A 417 (2006) 275–280.
[6] Z. Chen, Y. Lei, H. Zhang, Structure and properties of nanostructured A357 alloy produced by melt spinning compared with direct chill ingot, Journal of Alloys and Compounds 509 (2011) 7473–7477.
[7] M. Rajabi, A. Simchi, P. Davami, Microstructure and mechanical properties of Al–20Si–5Fe–2X (X = Cu, Ni, Cr) alloys produced by melt-spinning, Materials Science and Engineering A 492 (2008) 443–449.
[8] A. Aversa, M. Lorusso, G. Cattano, D. Manfredi, F. Calignano, E. P. Ambrosio, S. Biamino, P. Fino, M. Lombardi, M. Pavese, A study of the microstructure and the mechanical properties of an Al-Si-Ni alloy produced via selective laser melting, Journal of Alloys and Compounds, 25 (2017) 1470-1478.
[9] N. L. TAWFIK, Mechanical properties of rapidly solidified ribbons of some AI–Si based alloys, JOURNAL OF MATERIALS SCIENCE 32 (1997) 2997-3000.
[10] E. Karakose, T. Karaaslana, M. Keskina, O. Uzunc, Microstructural evolution and microhardness of a melt-spun Al–6Ni–2Cu–1Si (in wt.%) alloy, journal of materials processing technology 195 (2008) 58–62.
[11] Sung-Hwan Choi, Si-Young Sung, Hyun-Joo Choi, Young-Ho Sohn, BumSuck Han, Kee-Ahn Lee, High temperature tensile deformation behaviour of new heat resistant aluminium alloy. Procedia Engineering, 10 (2011) 159-164.